International Journal of Mass Spectrometry 275 (2008) 45–54

Contents lists available at ScienceDirect

International Journal of Mass Spectrometry

journal homepage: www.elsevier.com/locate/ijms

Atmospheric pressure photoionization mass spectrometry as a tool for the investigation of the hydrolysis reaction mechanisms of phosphite antioxidants

M. Papanastasiou[a], A.W. McMahon[b], N.S. Allen[a,*], B.W. Johnson[c], K. Keck-Antoine[c], L. Santos[d,1], M.G. Neumann[d]

[a] Manchester Metropolitan University, Department of Chemistry and Materials, Center for Materials Science, Chester Street, Manchester M1 5GD, UK
[b] University of Manchester, Wolfson Molecular Imaging Centre, 27 Palatine Road, M20 3LJ, UK
[c] Chemtura, Toekomstlaan 13, B-2200 Herentals, Belgium
[d] Instituto de Quimica de Sao Carlos, Universidade de Sao Paulo, Caixa Postal 780, 13560-970 Sao Carlos SP, Brazil

ARTICLE INFO

Article history:
Received 8 January 2008
Received in revised form 7 May 2008
Accepted 10 May 2008
Available online 18 May 2008

Keywords:
Dopant assisted-atmospheric pressure photoionization
Mass spectrometry
Phosphite antioxidants
Hydrolysis

ABSTRACT

The hydrolysis reaction mechanism of phosphite antioxidants is investigated by liquid chromatography-mass spectrometry (LC/MS). The phosphites were chosen because they differed in chemical structure and phosphorus content. Dopant assisted-atmospheric pressure photoionization (DA-APPI) is chosen as the ion source for the ionization of the compounds. In our previous work, DA-APPI was shown to offer an attractive alternative to atmospheric pressure chemical ionization (APCI) since it provided background-ion free mass spectra and higher sensitivity [M. Papanastasiou, et al., Polymer Degradation and Stability 91 (11) (2006) 2675–2682]. In positive ion mode, the molecules are generally detected in their protonated form. In negative ion mode, the phosphites are unstable and only fragment ions are observed; these however, are characteristic of each phosphite and may be used for the identification of the analytes in complex mixtures.

The analytes under investigation are exposed to accelerated humid ageing conditions and their hydrolytic pathway and stability is investigated. Different substituents around the phosphorus atom are shown to have a significant effect on the stability of the phosphites, with phenol substituents producing very hydrolytically stable structures. Alkanox P24 and PEP-36 follow a similar hydrolytic pathway via the scission of the first and then the second P—O_{phenol} bonds, eventually leading to the formation of phenol, phosphorous acid and pentaerythritol as end products. HP-10 exhibits a rather different structure and the products detected suggest scission of either the P—$O_{hydrocarbon}$ or one of the P—O_{phenol} bonds. A phenomenon similar to that of autocatalysis is observed for all phosphites and is attributed to the formation of dialkyl phosphites as intermediate products.

1. Introduction

Polymers, during their lifetime, are subjected to a number of degradation-initiating influences that result in the change, or even loss of their chemical and/or physical properties [2]. The need for chemical agents that would confer significant improvements on their properties has been evident since the very early stages of the polymer industry. These chemical agents are known as stabilizers and are incorporated into the polymer matrix at relatively low concentrations to combat degradation processes. For example, synergistic mixtures of primary hindered phenols with phosphorus-based secondary antioxidants are one of the most effective stabilizing systems, widely used in the processing stabilization and long-term application of polyolefins. Hindered phenols are well known in the literature as excellent *H*-donors [3–5]. The key mechanism by which they react is their donation of a *H*-atom to peroxy radicals to form hydroperoxides and the relatively stable phenoxy radicals. The hydroperoxides formed are in turn decomposed by phosphites in a non-radical way [5].

A major drawback, however, is that in the presence of small amounts of water or moisture, phosphites hydrolyze to give their respective phosphonate forms. Positive and negative effects of this process have been reported. In terms of their functionality for effective polymer stabilization, better results were obtained by the use of combined systems of hydrolysable and non-hydrolysable phosphates [6]. Hindered phenols released during hydrolysis form synergistic mixtures with either the parent phosphite, or its inter-

* Corresponding author. Tel.: +44 161 247 1432; fax: +44 161 247 6332.
E-mail address: n.s.allen@mmu.ac.uk (N.S. Allen).
[1] Visiting Researcher from Sao Carlos University, Brazil.

1387-3806/$ – see front matter © 2008 Elsevier B.V. All rights reserved.
doi:10.1016/j.ijms.2008.05.012

mediate hydrolysis products and these contribute to the overall stabilization performance through chain terminating mechanisms [6,7]. Hydrolysis products were also found to be active processing stabilizers themselves by preventing discoloration and enhancing melt stabilization of the polymer [8]. Negative effects concern handling issues of the phosphites since, when hydrolyzed, they tend to cake and become sticky. Also, corrosion of the processing equipment might be caused due to the formation of acidic products during the processing [9]. Finally, special precautions must be taken during storage to avoid degradation of the compounds [10].

In our previous work, the hydrolysis reaction mechanism of bis(2,4-di-*tert*-butylphenyl)pentaerythritol diphosphite (Alkanox P24) was investigated by FTIR [8] and the anticipated intermediates and products in the hydrolytic pathway of the phosphite were investigated by LC/MS means [1]. It was shown that hydrolysis of the phosphite proceeded via the scission of the P—O_{phenol} bonds to yield 2,4 di-*tert*-butyl phenol and pentaerythritol as final products. A number of intermediate products were also identified. For the ionization of the phosphites prior to mass spectrometric analysis, the applicability of the DA-APPI was assessed and compared to that of APCI. DA-APPI was developed in the year 2000 as an alternative to electrospray ionization (ESI) and APCI to allow the successful ionization of low to non-polar analytes [11]. APPI nowadays has evolved into an important interface for LC/MS, reflected probably to the rapidly growing number of applications in this field [12].

So far, ESI and APCI have been the methods of choice for additive analysis [13–21]. Brominated flame retardants, used in a variety of consumer and industrial products, have been successfully analyzed by HPLC/ESI/MS in biological fluids [16] and tissue samples [13,14]. HPLC/APCI/MS has also been applied to the same group of compounds for their analysis in plastics [18], where the performance of APPI has been assessed for their characterization and degradation pathways in synthetic mixtures [22]. Ionization mechanisms taking place in the ion source were investigated in the latter case and were similar to those previously reported for related structures [23]. Other applications involved the analysis of common antioxidants, slip agents and light stabilizers by SFC/APCI/MS [17] and HPLC/APCI/MS [15,19]. A few applications in the field also deal with the characterization of additives and their degradation pathways [20,21,24–27]. It would therefore seem appropriate to pursue the study of antioxidant hydrolysis with the same promising DA-APPI ionization technique.

In this study, the hydrolytic pathway of the phosphites PEP-36 (ADEKA, Japan), HP-10 (ADEKA, Japan) and Alkanox 28 (Chemtura, Italy) was investigated and on the basis of the mass spectrometry, reaction schemes were derived. The analytes were exposed to accelerated humid ageing conditions and the hydrolysis products were analyzed by LC/MS means using DA-APPI. Different hydrolytic stabilities were observed and exhibited dependence on the substituents around the phosphorus atom.

Table 1
Phosphite antioxidants and respective monoisotopic masses

Phosphite antioxidants	Structures
Alkanox P24 (Bis(2,4-di-*tert*-butylphenyl) pentaerythritol diphosphite) $C_{33}H_{50}P_2O_6$ MM[a] 604.31 amu	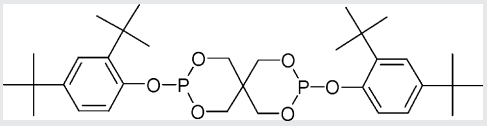
PEP-36 (Bis(2,6-di-*tert*-butyl-4-methylphenyl) pentaerythritol diphosphite) $C_{35}H_{54}P_2O_6$ MM 632.34 amu	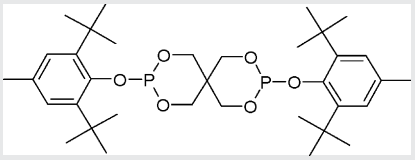
Alkanox 28 (Bis(2,4-dicumylphenyl) pentaerythritol diphosphite) $C_{53}H_{58}P_2O_6$ MM 852.37 amu	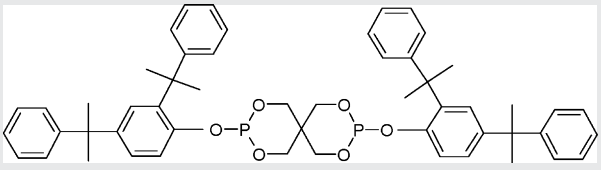
HP-10 (2,2-methylenebis(4,6-di-*tert*-butylphenyl) octylphosphite) $C_{37}H_{59}PO_3$ MM 582.42 amu	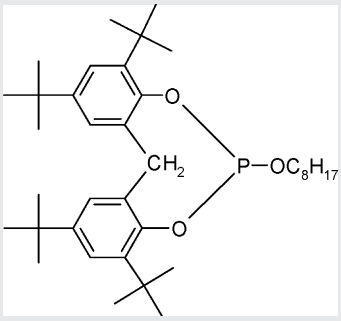

[a] MM = monoisotopic mass.

2. Experimental

2.1. Chemicals and reagents

Alkanox P24 and Alkanox 28 were supplied from Chemtura Corporation (Herentals, Belgium). PEP-36 and HP-10 were supplied from ADEKA Argus (Saitama, Japan). The structures of the phosphites along with their monoisotopic masses are featured in Table 1. Acetonitrile and isopropanol were HPLC grade (≥99.9% and ≥99.8%, respectively, BDH Laboratory Supplies, Poole, UK). Toluene HPLC grade was supplied by Aldrich (98%, Dorset, UK). Sodium chloride was supplied by Lancaster (Morecambe, UK).

2.2. Instrumentation

Mass spectra were collected with the API 365 (Applied Biosystems/MDS Sciex) using the DA-APPI ion source. Vaporized liquid nitrogen (Cryospeed, Lancashire) was used as the nebulizer gas, the curtain gas, the collision gas and the lamp gas in the APPI ion source. For infusion experiments, the phosphite solutions were delivered with a Harvard Apparatus syringe pump. A second pump (binary PerkinElmer Series 200 LC) was employed to deliver the HPLC-grade dopant toluene. Spectra were collected with the first quadrupole at a scan rate of 1 scan s^{-1}; 30 scans were averaged. The mass range acquired was 150–700 amu for PEP-36 and 200–700 amu for HP-10. When coupled to the HPLC (SIM mode), the acquisition time of the quadrupole was set at 200 ms for each ion.

For the optimization of the MS parameters, phosphite solutions of 1 mg L^{-1} were infused into the mass spectrometer at an optimum flow rate of 0.1 mL min^{-1} that produced a stable total ion current; the dopant was added at a flow rate ratio of 1:1. The ion source voltage (ISV) in DA-APPI was 1350 V, creating a current of ~0.7 mA. Source parameters such as the declustering and focusing potential, the temperature of the heated nebulizer and the nitrogen gas flow rates were optimized manually to provide maximum S/N for the protonated phosphites. The ion source potentials for the individual phosphites are given in Table 2; counter values were used in the negative ion mode analysis. The declustering potential was set preferably low to avoid 'in-source' fragmentation of the protonated phosphites. The flow rate of the nebulizer and curtain gas were 9 and 10 L min^{-1}, respectively. The temperature of the heated nebulizer was set at 475 °C. Similar gas flow rates and temperature were used in the analysis of the phosphites in negative ion mode.

For the separation of the hydrolysis products of the phosphites an Agilent 1100 HPLC system was utilized. The column was a Phenomenex Luna C18 (2), 150 mm × 4.6 mm, 3 μm. The flow rate for all phosphites was set at 1 mL min^{-1} and the column effluent was introduced to the mass spectrometer without the use of a splitter. The injection volume was 2 μL. The mobile phase consisted of acetonitrile and 2-propanol and isocratic runs were utilized. Their percentage ratios were as follows: Alkanox P24, ACN/2-propanol 50/50; HP-10, ACN/2-propanol 30/70 and PEP-36, ACN/2-propanol, 70/30. Water was not used in the mobile phase so as to avoid further hydrolysis of the products.

Table 2
Positive ion DA-APPI potentials for the phosphites under investigation; counter values were used in negative ion mode analysis

APPI	DP^+	FP^+	EP^+
HP10	11.7	100.5	4.2
Alkanox P24	19.8	89.5	3.9
PEP36	9.1	105.2	5.6
Alkanox 28	34.8	149.2	4.9

DP: declustering potential; FP: focusing potential; EP: entrance potential. $^+$Values expressed in volts.

2.3. Sample preparation

For the controlled hydrolysis experiments, samples of the phosphites were weighed (0.1 g) in glass vials (25 mL) and placed in a desiccator in an air circulating oven (Carbolite 60) at 70 °C. Water was added at the bottom of the desiccator to produce a relative humidity (R.H.) of 100% upon heating. Samples were removed from the oven periodically, dissolved in toluene/2-propanol (50/50) and further diluted to a final concentration of 5 mg L^{-1} for mass spectrometric analysis. When combined with HPLC, concentrations of 20 mg L^{-1} were prepared.

3. Results and discussion

3.1. Ionization of the phosphites by DA-APPI

DA-APPI is closely related to APCI, with the discharge needle being replaced commonly by a Krypton discharge VUV lamp that emits photons at a strong 10.0 eV line at 123.6 nm and a weaker (~1/10) 10.6 eV line at 116.5 nm [28]. The low energy of the photons has the obvious advantage of avoiding the ionization of species, such as components of air and common LC solvents that possess ionization energies (IE) higher than the energies of the photons. In DA-APPI the photons are absorbed by the dopant (solvent added in abundance to enhance the ionization efficiency) forming radical cations that in turn react with the analytes and LC solvents to form mainly protonated molecules and molecular radical cations [11]. In negative ion mode, the ionization of the analytes is believed to be initiated by the thermal electrons formed in the photoionization of the dopant [29,30]. Though the ionization mechanisms in this mode of analysis are not well defined, electron capture, charge exchange, proton transfer and substitution reactions have been reported to take place [30].

In our previous work, the ionization mechanisms of Alkanox P24 in both DA-APPI and APCI were explored [1]. In positive ion mode, Alkanox P24 gave mainly protonated molecules and few fragment ions corresponding to the elimination of tertiary butyl groups from the hindered phenol moieties. In negative ion mode, the molecular ion of the phosphite was unstable and only fragment ions were detected. In this work, solutions of 5 mg L^{-1} of the phosphites in toluene/2-propanol were prepared and infused to the mass spectrometer at a flow rate of 0.1 mL min^{-1}. Toluene was co-infused as the dopant. The structures of the phosphites under investigation along with their monoisotopic masses are depicted in Table 1.

Both PEP-36 and Alkanox 28 are symmetrical diphosphites with different substituent groups around the phosphorus atoms. The molecules are highly symmetrical and like Alkanox P24, two equivalent P—O_{phenol} and four equivalent P—$O_{pentaerythritol}$ bonds can be distinguished [31]. For PEP-36, in positive ion mode, the base peak corresponded to the $[M+H]^+$ protonated molecule detected at *m/z* 633.5 (Fig. 1). Despite a low declustering potential of 9.1 V, the phosphite fragmented giving many different ion species. The ion at *m/z* 577.6 was attributed to the loss of a *tert*-butyl group (56 amu) from the parent phosphite. Loss of a 2,6-di-*tert*-butyl-4-methyl phenol (BHT) from the $[M+H]^+$ resulted in the ion detected at *m/z* 431.6 and the respective phenol related ions at *m/z* 220.5 as shown in the figure. In negative ion mode, no molecular ion was detected and the phosphite exhibited two major fragment ions detected at *m/z* 218.9 and *m/z* 445.6 (Fig. 2). The former corresponded to the deprotonated molecule $[M-H]^-$ of BHT and has also been detected in the analysis of similar phosphite antioxi-

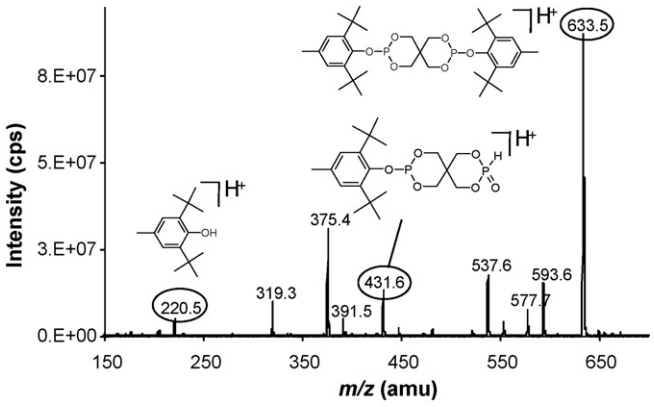

Fig. 1. Positive ion spectrum of PEP-36; the protonated molecule of the phosphite is detected at *m*/*z* 633.5.

dants and related phenols in negative ion APCI mode [17,32]. MS/MS of this ion yielded only one fragment ion detected at *m*/*z* 202.9, corresponding to a methane loss from the deprotonated molecule [32]. As mentioned in the analysis of the phosphite in positive ion mode, loss of a BHT molecule from the parent phosphite resulted in the ion detected at *m*/*z* 431.6. In negative ion mode, only its oxidation products ($[M-H+O]^-$ and $[M-H+2O]^-$) at *m*/*z* 445.6 and *m*/*z* 461.8 were detected, indicating that the fragment of the phosphite oxidized readily to produce the respective phosphonate forms (Fig. 2). MS/MS analysis of both of these ions yielded fragments at *m*/*z* 218.9 and *m*/*z* 79 corresponding to the $[M-H]^-$ of BHT and to the PO_3^-, respectively. The ionization of Alkanox 28 was similar to that of PEP-36 (spectra not shown here). In positive ion mode, the $[M+H]^+$ ions were detected at *m*/*z* 853.7 indicating proton transfer reactions between the phosphite and the dopant radical cations. In negative ion mode, two fragment ions were detected at *m*/*z* 329.4 and *m*/*z* 555.6. The former corresponded to the deprotonated molecule $[M-H]^-$ of 2,4-dicumylphenyl group (monoisotopic mass, 330.2 amu), whereas the latter corresponded to the oxidation product of the ion formed with the loss of the 2,4-dicumylphenyl group from the parent phosphite.

Overall, the analyses of PEP-36 and Alkanox 28 in positive and negative ion modes showed similar behaviors to those of Alkanox P24. The base peak in positive ion mode corresponded to the protonated phosphites. In negative ion mode, the phosphites were unstable and only fragment ions were detected originating from the loss of phenol molecules followed by reactions with O_2 molecules.

The structure of HP-10 differs rather significantly from the phosphites analyzed so far in terms of phosphorus content, symmetry

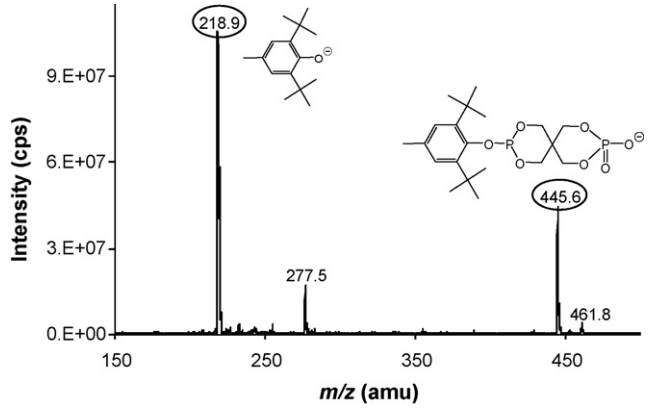

Fig. 2. Negative ion spectrum of PEP-36; the phosphite is unstable and only fragment ions are detected.

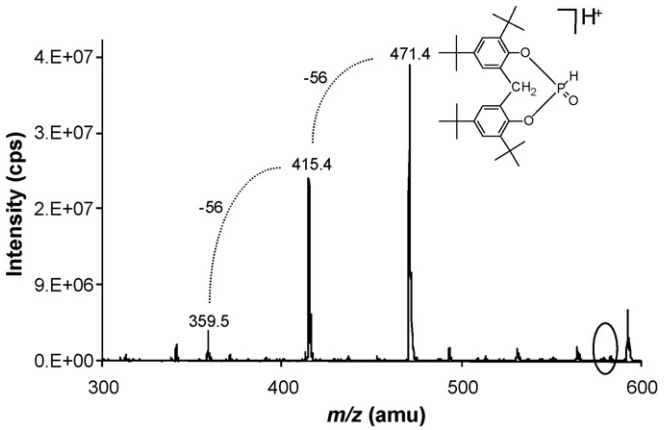

Fig. 3. Positive ion spectrum of HP-10; the base peak is produced by the loss of the hydrocarbon chain from the parent phosphite.

and substitution groups. HP-10 contains both phenol moieties as well as a rather small hydrocarbon chain. The positive ion spectrum of HP-10 is presented in Fig. 3. The protonated molecule was unstable and only fragment ions were detected. Loss of the hydrocarbon chain (C_8H_{17}) from the parent phosphite yielded ions at *m*/*z* 471.4. MS/MS of this ion produced fragments at *m*/*z* 415.4 and *m*/*z* 359.5, corresponding to two consecutive losses of *tert*-butyl groups (56 amu) from the phenol moieties. In negative ion mode no molecular ion was detected, however, unlike the pentaerythritol diphosphites that showed only fragment ions, HP-10 exhibited peaks at higher *m*/*z* ratios (Fig. 4). The peak at *m*/*z* 597.6 was assigned as the oxidation product ($[M-H+O]^-$) of the $[M-H]^-$ ion of the phosphite (monoisotopic mass, 582.42). The *m*/*z* 629.8 ion exhibited a difference of 32 masses with the 597.6 ion, indicating reactions of this ion with oxygen molecules. Since the phosphorus atom was already in the phosphonate form, the oxygen atoms were expected to oxidize the phenol moieties giving presumably the respective quinines [33]. Collisional fragmentation of the *m*/*z* 629.8 ion showed losses of the hydrocarbon chain as well as of DTBP molecules. The base peak detected at *m*/*z* 421.6 was likely to correspond to the $[M-H]^-$ ion of structure (E) drawn in Fig. 9 with further loss of a H_2 molecule.

3.2. Hydrolysis mechanism of PEP-36

It is well known in the literature that common phosphites undergo hydrolysis when exposed to small amounts of water [2] In this section, the controlled hydrolysis experiments carried out with

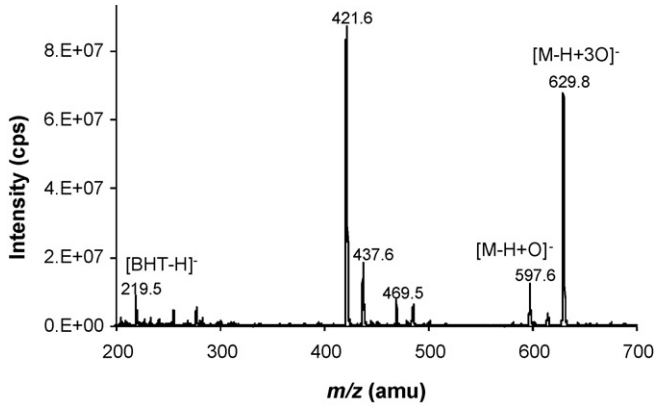

Fig. 4. Negative ion spectrum of HP-10; oxidation products as well as fragment ions of the parent phosphite are observed.

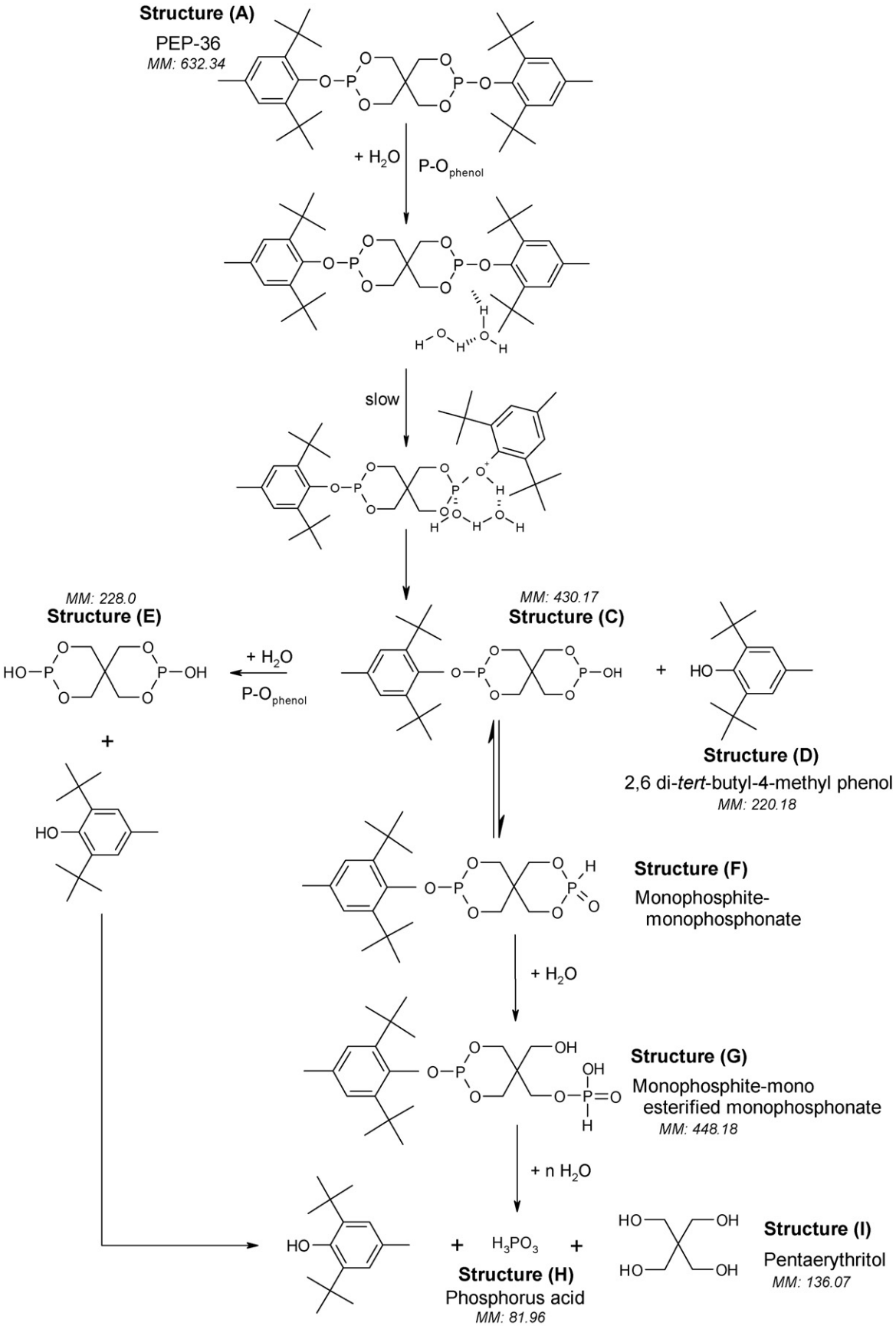

Fig. 5. Hydrolysis reaction mechanism of PEP-36 (see text for details).

the PEP-36 and HP-10 are discussed. The phosphites were exposed at temperatures <100 °C because at higher temperatures, phosphites are known to degrade rapidly and decay via oxidation [34]. Positive and negative ion DA-APPI was utilized since depending on their functional groups, degradation products of the phosphites were ionized selectively in either mode of analysis. MS/MS was employed for qualitative investigations of the products formed and HPLC was interfaced online for the separation of the hydrolysis products.

A brief discussion of the theory underlying the hydrolysis mechanism of the phosphites was given in our previous work and the products proposed in the hydrolytic pathway of Alkanox P24 [8] were confirmed by mass spectrometry [1]. It was shown that hydrolysis proceeded via the cleavage of one of the P—O_{phenol} bonds from the parent phosphite, with subsequent loss of a 2,4 di-*tert*-butyl phenol molecule (DTBP). In the subsequent stage of hydrolysis the phosphorinane ring opened forming the monophosphite-mono esterified monophosphonate that was unstable and yielded phosphorous acid, DTBP and pentaerythritol as final products. In the early stages of hydrolysis, scission of the second P—O_{phenol} bond was also observed giving rise to pentaerythritol diphosphite and DTBP. At advanced stages of hydrolysis, scission of the P—$O_{pentaerythritol}$ bond, as proposed in the literature to occur, was not observed [10]. Like Alkanox P24, PEP-36 is a symmetrical diphosphite and was expected to follow a similar hydrolysis pathway. The hydrolysis scheme is drawn in Fig. 5; the monoisotopic masses of the intermediate and final products are also given.

For the PEP-36 hydrolysis experiments, the samples were introduced into the oven at 70 °C and at 100% R.H. The first quadrupole was set to scan over the range of 30–700 amu and the mass spectra were collected over time in both positive and negative ion modes. An isocratic run of 70/30 acetonitrile/2-propanol was utilized to elute the compounds and introduce them to the mass spectrometer at a flow rate of 1 mL min^{-1}. For the first eight hours and under these oven conditions, no hydrolysis products were observed, suggesting that the phosphite was more stable than Alkanox P24 that hydrolyzed within the first hour [1]. In Fig. 6, the positive and negative ion chromatograms of a sample that was removed at 10 h are

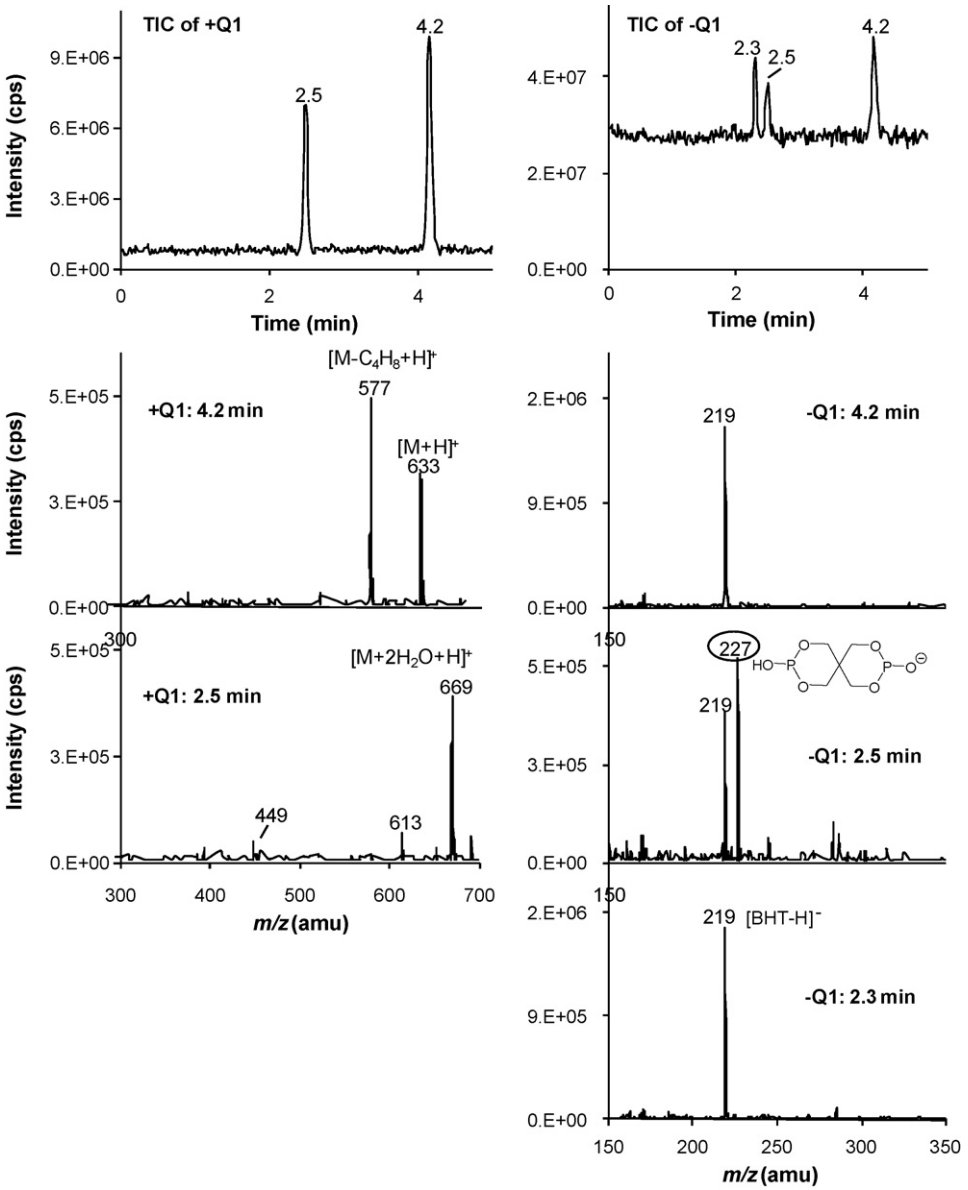

Fig. 6. Positive and negative ion chromatograms and respective spectra of the '10 h sample (70 °C, 100% R.H.) of PEP-36.

presented, along with their respective mass spectra. In the positive ion mode, two peaks were observed at 4.2 and 2.5 min. The former was assigned to the parent phosphite. Its positive ion mass spectrum showed two major ions corresponding to the $[M+H]^+$ (*m*/*z* 633) and a fragment ion originating from the loss of a *tert*-butyl group (*m*/*z* 577) from the parent molecule. In negative ion mode, the phosphite was unstable and only the $[M-H]^-$ ion of BHT (*m*/*z* 219) was detected. The positive ion mass spectrum of the 2.5 min showed ions at *m*/*z* 669, *m*/*z* 613 and *m*/*z* 449. The first peak corresponded to the parent phosphite with absorption of two molecules of water, giving the $[M+2H_2O+H]^+$ ion. Loss of a *tert*-butyl group produced the *m*/*z* 613 ion, whereas loss of a BHT phenol molecule, the *m*/*z* 449 ion. Similar losses were observed in the hydrolysis of Alkanox P24 for the *m*/*z* 641 that was assigned as the $[M+2H_2O+H]^+$ ion. The negative ion mode analysis of the 2.5 min peak revealed two major ions detected at *m*/*z* 219 and *m*/*z* 227, the former corresponding to the $[M-H]^-$ ion of BHT. The *m*/*z* 227 ion corresponded to the deprotonated pentaerythritol diphosphite (its structure is shown in Fig. 5, structure (E)). MS/MS was employed to investigate the fragmentation pattern of this ion and compare it with the fragmentation pattern of a same mass ion detected as a hydrolysis product in the analysis of Alkanox P24 [1]. The fragment ions were similar arising from losses of HPO_2 and HCHO giving ions at *m*/*z* 163 and *m*/*z* 133, respectively. Phosphite ions at *m*/*z* 79 (PO_3^-) and *m*/*z* 63 (PO_2^-) were also detected (data not shown here). PO_3^- was the base peak in both spectra. It was concluded therefore that the *m*/*z* 227 ion was produced in the hydrolysis of both phosphites and originated from the scission of both $P-O_{phenol}$ bonds from the parent molecules. Finally, the negative ion spectrum of the 2.3 min peak revealed only one major ion at *m*/*z* 219, assigned to the $[M-H]^-$ of BHT. The formation of phenols as final hydrolysis products of phosphites is well established in the literature [35]. Another sample was removed and analyzed at 11 h; at this stage, hydrolysis seemed to be complete, since the parent phosphite was not present and deprotonated BHT was the only peak detected. Similar results were obtained for the samples removed from the oven for $t > 11$ h.

The evidence, therefore, suggested that after the hydrolysis was initiated, at the given oven conditions (70 °C, 100% R.H.), it proceeded rapidly via the scission of both $P-O_{phenol}$ bonds to produce the pentaerythritol diphosphite (structure (E)). This intermediate hydrolyzed further to produce pentaerythritol and phosphorous acid. BHT was detected as a final hydrolysis product. It was presumed, therefore, that PEP-36 followed a similar hydrolysis pathway with Alkanox P-24, despite the fact that under the oven conditions employed, intermediates (structures (C), (F), and (G) in Fig. 5) were not detected. The rapid completion of the hydrolysis reaction, following initiation, suggested that reactive intermediates, similar to those of Alkanox P24 were formed that catalyzed the reaction; their formation is still to be proven.

3.3. Hydrolysis mechanism of HP-10

For the HP-10 hydrolysis experiments, similar oven conditions to those used with PEP-36 were employed (70 °C, 100% R.H.). The first quadrupole was set to scan over the range of *m*/*z* 30–650. The mobile phase consisted of acetonitrile/2-propanol at a ratio of 30/70. In Fig. 7, the positive total ion chromatogram and the respective mass spectrum of a non-hydrolyzed sample of the phosphite are depicted. Under the current HPLC conditions, the phosphite eluted at 9.1 min. Its mass spectrum showed two major fragment ions at *m*/*z* 554 and *m*/*z* 471, the former originating from the loss of C_2H_4 presumably from the hydrocarbon chain of the parent phosphite whereas the latter arose from the loss of the entire hydrocarbon chain C_8H_{17}. The $[M+H]^+$ ion at *m*/*z* 583 was present at very low abundance. Compared to the positive ion spectrum of the phosphite by infusion (Fig. 3), different ratios of the ions have been obtained, attributed probably to the presence of acetonitrile in the mobile phase. Experimental data [36] and semi-empirical calculations [37] have shown that upon photon irradiation of acetonitrile, isomers are produced that possess ionization potential lower than 10 eV, consequently participating in the ionization of the analytes. In negative ion mode, the phosphite exhibited a very poor signal and is not shown here.

Hydrolysis products were detected within a period of 3 h after the samples were introduced to the oven. The phosphite, however, was the base peak for a fairly long period and its intensity decreased rapidly after 27 h oven ageing time, followed by the rapid increase of its hydrolysis products. In Fig. 8, the negative ion analysis of a sample that was removed from the oven at '$t = 36$ h' is chosen to be shown due to the high intensity of the hydrolysis products. The hydrolysis products were also detected in positive ion mode, but their ionization efficiency was very poor. For '$t = 36$ h', the intensity of the parent phosphite in positive ion mode was very low, indicating that hydrolysis was almost complete. Three additional chromatographic peaks were detected in negative ion mode, at 2.7, 3 and 5.3 min. The first peak produced a major ion at *m*/*z* 469 assigned to the loss of the hydrocarbon chain from the parent phosphite, forming structure (B) (Fig. 9). The two peaks eluting at 3.0 and 5.3 min produced similar spectra with ions detected at *m*/*z* 424. The former was likely to originate from the scission of both $P-O_{phenol}$ bonds of the phosphite forming structure (E) (Fig. 9). MS/MS of this ion produced intense ions at *m*/*z* 205 solely. The *m*/*z* 205 corresponded to the $[M-H]^-$ of DTBP, verifying therefore the presence of the hindered phenol moieties in the molecule. The ion eluting at 5.3 min was consistently of lower abundance than the ion eluting at 3.0 min and collisional fragmentation experiments failed to produce characteristic fragment ions that would allow conclusions for its structure to be drawn. The similar spectra of these two peaks however may suggest the formation of an isomer of structure (E), but this hypothesis is being explored in more detail in further studies. Both

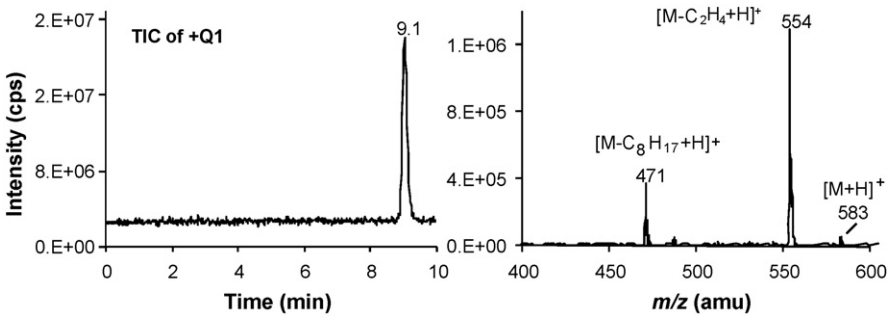

Fig. 7. Positive ion analysis of a non-hydrolyzed sample ($t = 0$) of HP-10.

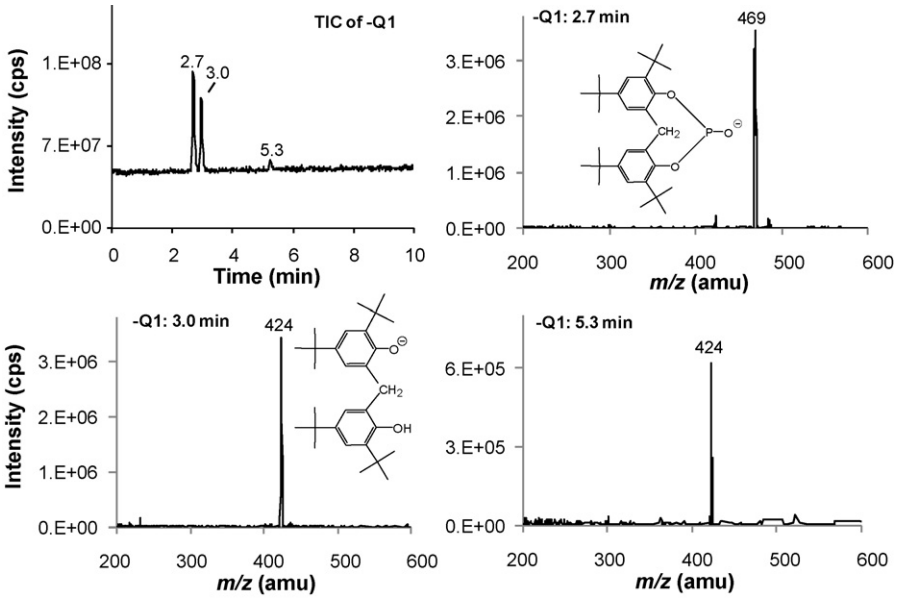

Fig. 8. Negative ion analysis of a '36 h' sample (70 °C, 100% R.H.) of HP-10.

of the structures (B) and (E) were very stable over time after these had been formed and were detected as final hydrolysis products.

Based on these results, a hydrolysis scheme is tentatively proposed and is shown in Fig. 9. Similarly, as with the other phosphites, hydrolysis started with an electrophilic attack of the water hydrogen on the phosphorus atom and resulted in the scission of one of the P—O bonds. The evidence suggested that it was the $P—O_{hydrocarbon}$ bond producing structure (B) (*m*/*z* 469) and not one of the $P—O_{phenol}$ bonds. The peaks corresponding to the degradation products, however, appeared at the same time suggesting some sort of equilibrium between structure (B) and structure (E). Both of them exhibited similar intensity trends throughout the experiment; a rather low abundance at the beginning until the rapid decrease of the phosphites' concentration that led to an analogous steep increase of the peak areas of the hydrolysis products. Structure (B) was very stable throughout the experiment and did not hydrolyze further. This led us to assume that an alternative hydrolysis pathway may be followed through the scission of one of the $P—O_{phenol}$ bonds to form structure (F). The hydrolysis of the tautomer (structure (G)) might have produced either the monophosphonate form (structure (D)) through the scission of the $P—O_{hydrocarbon}$ bond, or structure (E) through the scission of the second $P—O_{phenol}$ bond. There was no evidence, however, for the formation of structures (F) and (G) since respective molecular ion peaks were not detected and their formation is to be investigated in future work.

Hydrolysis of HP-10 started within the first three hours after the samples were introduced to the oven; however, the process appeared to be slow for several hours. The peak area of the phosphite decreased slowly over time, but exhibited a steep decline between 27 and 29 h. As with the previous phosphites under investigation, this was attributed to the formation of dialkyl phosphites. Their presence in the reaction mixture is expected to have an acceleration effect on the rate of hydrolysis [38].

3.4. Overview of hydrolysis

Controlled hydrolysis experiments were carried out with phosphite antioxidants of different structures in order to assess their hydrolytic stabilities and identify possible hydrolysis products. Alkanox P24 (presented in our previous paper), PEP-36 and HP-10 were hydrolyzed successfully at 70 °C and 100% R.H, whereas Alkanox 28 showed excellent hydrolytic stability and was not hydrolyzed under the current oven conditions.

For Alkanox P24 and PEP-36 that were of similar structure, the results suggested that the phosphites followed a similar hydrolysis pathway mainly by the splitting of the first and then of the second $P—O_{phenol}$ bonds to yield pentaerythritol diphosphite as an intermediate and phenol, pentaerythritol and phosphorous acid as final products. The last two substances were detected in the hydrolysis reaction mechanism of Alkanox P24 by FTIR studies in previous work [8]. We, therefore, presumed their presence as end products also in the hydrolysis mechanism of PEP-36. Hydrolysis of the phosphites through the scission of the $P—O_{pentaerythritol}$ bond was not observed for any of the structures since the hydrolytic resistance of the P—O—C bond in the pentaerythritol fragment is higher than that of the bond in the monophenol fragment [39].

HP-10 that contained only one phosphorus atom exhibited a rather different behavior with the splitting of the aliphatic hydrocarbon chain from the parent molecule. This structure was shown to be in equilibrium with the phenol moiety that was expected to be detected as a final hydrolysis product. This probably indicated an alternative hydrolysis pathway through the scission of one of the $P—O_{phenol}$ bonds eventually leading to the phenol moiety (structure (E), Fig. 10) with further hydrolysis. However, this alternative route, through the formation of structures (F) and (G), is to be investigated in future work by using milder oven conditions.

The hydrolytic stabilities of the three phosphites are depicted in Fig. 10. The figure was constructed by monitoring the HPLC peak area of the parent phosphites over the oven ageing time. The degree of hydrolysis was then calculated as a percentage of the measured area depletion of the parent phosphites. For instance, the degree of hydrolysis at '0 min', where no hydrolysis has occurred, is zero. According to the literature, the steric hindrance around the phosphorus atom results in higher hydrolytic stability [40–42]. Alkanox P24 with only one *tert*-butyl group around the phosphorus atom exhibited the lowest hydrolytic stability, and was hydrolyzed in less than four hours, whereas the two *tert*-butyl groups of PEP-36 exhibited a significant effect on the hydrolytic stability of the latter. Alkanox 28 with substituted phenols instead of *tert*-butyl groups exhibited the highest hydrolytic stability. HP-10 that was structurally different exhibited a rather low sensitivity towards

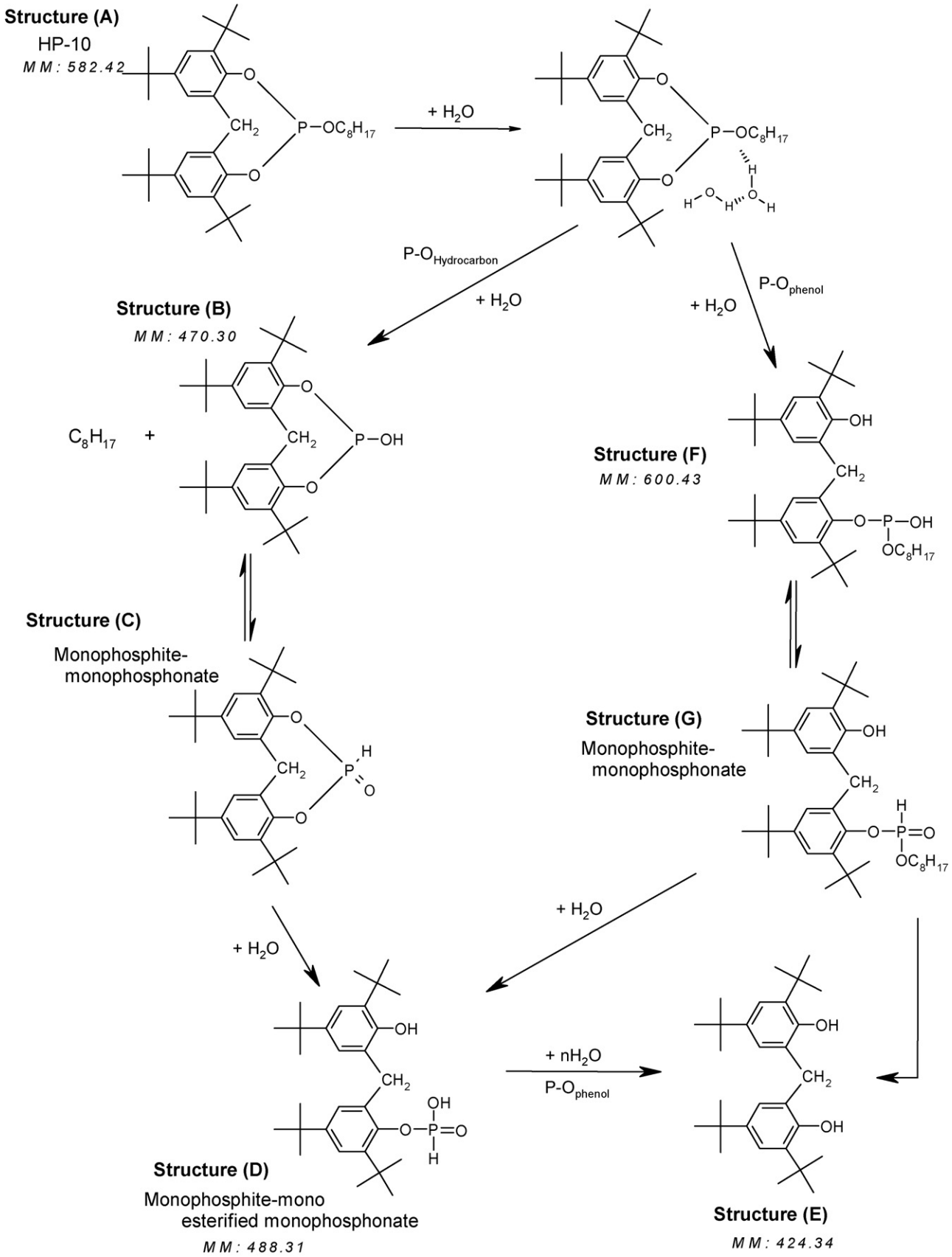

Fig. 9. Hydrolysis reaction scheme of HP-10 (see text for details).

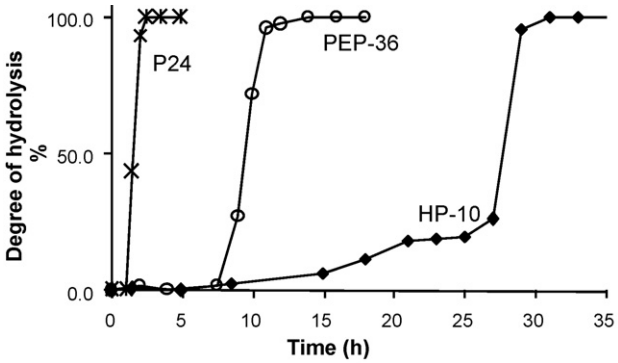

Fig. 10. Degrees of hydrolysis of Alkanox P24, PEP-36 and HP-10.

hydrolysis, probably attributed to the two phenol moieties that it contained; these were expected to reduce the electron density at the phosphorus atom, and, therefore, to increase its hydrolytic stability [42]. An effect equivalent to autocatalysis, explained in the literature more as a solubilising effect, was observed for all three structures and was attributed to the formation of dialkyl phosphites as intermediates [38,43]. In contrast to trialkylphosphites, dialkylphosphates are soluble in water; this leads to more rapid diffusion of water vapor into the phosphate based mixture, resulting in an increase to the rate of hydrolysis.

4. Conclusions

DA-APPI was chosen for the analysis of phosphite antioxidants of different chemical structures and phosphorus content. The ion formation characteristics were briefly discussed. In positive ion mode the protonated analyte was generally detected, whereas in negative ion mode, no intact molecular or pseudomolecular ions were observed. The phosphites were unstable and only fragment ions were detected; these however were characteristic of each phosphite and may be used for the identification of the analytes in complex mixtures. Substitution reactions were also observed in this mode of analysis.

The phosphites were exposed to accelerated humid ageing conditions and their hydrolytic stability was investigated. Different substituents around the phosphorus atom had a significant effect on the stability of the phosphites with Alkanox P24 being the least stable. Phenol substituents (Alkanox 28) were shown to increase the stability of the phosphite dramatically. Alkanox P24 and PEP-36 followed a similar pathway with the scission of the first and then the second P—O_{phenol} bonds, eventually leading to the formation of phenol, phosphorous acid and pentaerythritol as end products. HP-10 exhibited a rather different structure and the products detected suggested scission of either the P—$O_{hydrocarbon}$ or one of the P—O_{phenol} bonds. A phenomenon similar to that of autocatalysis was observed for all phosphites attributed to the formation of dialkyl phosphites as intermediate products. Dialkyl phosphites are known to be very reactive and their formation is to be investigated in future work by using milder oven conditions.

Acknowledgements

The authors gratefully acknowledge Chemtura, Belgium for sponsoring this project. The authors also feel indebted to Applied Biosystems/MDS Sciex and GlaxoSmithKline for their support and a visiting scholarship to LS to Fapesp (No. 04/02112) and Capes (No.4491-05-0).

References

[1] M. Papanastasiou, N.S. Allen, B. Johnson, K. Keckant-Antoine, A. Mcmahon, Polymer Degradation and Stability 91 (11) (2006) 2675.
[2] W.D. Habicher, I. Bauer, in: H.S. Halim (Ed.), Handbook of Polymer Degradation, Marcel Dekker, New York, 2000, p. 81.
[3] K. Schwarzenbach, B. Gilg, D. Muller, G. Knobloch, J.R. Pauquet, P. Rota-Graziosi, A. Schmitter, J. Zingg, in: Z. Hans (Ed.), Plastics Additives Handbook, Munich, Hanser, 2001, p. 1.
[4] G. Scott, Antioxidants: radical chain-breaking mechanisms, in atmospheric oxidation and antioxidants, Elsevier Publishing Company, 1965, p. 115.
[5] W.D. Habicher, I. Bauer, J. Pospisil, Macromolecular Symposia 225 (1) (2005) 147.
[6] J. Tochacek, J. Sedlar, Polymer Degradation and Stability 41 (2) (1993) 177.
[7] K. Schwetlick, J. Pionteck, A. Winlker, U. Hahner, H. Koroschwitz, W.D. Habicher, Polymer Degradation and Stability 31 (2) (1991) 219.
[8] N. Ortuoste, N.S. Allen, M. Edge, B. Johnson, K. Keckant-Antoine, Polymer Degradation and Stability 91 (1) (2006) 195.
[9] M. Minagawa, Polymer Degradation and Stability 25 (2–4) (1989) 121.
[10] J. Tochacek, J. Sedlar, Polymer Degradation and Stability 50 (3) (1995) 345.
[11] D.B. Robb, T.R. Covey, A.P. Bruins, Analytical Chemistry 72 (15) (2000) 3653.
[12] S.J. Bos, S.M. van Leeuwen, U. Karst, Analytical and Bioanalytical Chemistry 384 (1) (2006) 85.
[13] W. Budakowski, G. Tomy, Rapid Communications in Mass Spectrometry 17 (13) (2003) 1399.
[14] G.T. Tomy, W. Budakowski, T. halldorsa, L. Kaj, K. Stromberg, E. Brorstrom-Lunden, Environmental Science and Technology 38 (8) (2004) 2298.
[15] J.P. Jaeg, E. Perdu, L. Dolo, L. Debrauever, J.P. Cravedi, D. Zalko, Journal of Agricultural and Food Chemistry 52 (2004) 4935.
[16] T. Hayama, H. Yoshia, S. Onimaru, S. Yonekawa, H. Kuroki, Journal of Chromatography B 809 (1) (2004) 131.
[17] M.J. Carrott, G. Davidson, The Analyst 123 (1998) 18.
[18] M. Schlummer, L. Gruber, A. Maurer, G. Wolz, R. van Eldik, Journal of Chromatography A 1064 (1) (2005) 39.
[19] C. Block, L. Wynants, M. Kelechtermans, R. de Boer, F. Comperrolle, Polymer Degradation and Stability 91 (12) (2006) 3163.
[20] X.Z. Xiang, J. Dahlgren, W.P. Enlow, A.G. Marshall, Analytical Chemistry 64 (22) (1992) 2862.
[21] H. El Mansouri, N. Yagoubi, D. Ferrier, Chromatographia 48 (7–8) (1998) 491.
[22] L. Debrauwer, S. Chevolleau, P. Zalko, A. Paris, J. Tulliez, Journal of Chromatography A 1082 (1) (2005) 98.
[23] E. Basso, E. Marrotta, R. Seraglia, M. Tubarov, P. Traldi, Journal of Mass Spectrometry 38 (10) (2003) 1113.
[24] K. Moller, U. Nilsson, C. Crescenzi, Journal of Chromatography A 938 (1–2) (2001) 121.
[25] K. Nagy, E. Epacher, P. Staniek, B. Pukanszky, Polymer Degradation and Stability 82 (2) (2003) 211.
[26] J. Scheirs, S.W. Bigger, O. Delatycki, Polymer Durability, 1996, p. 359.
[27] M. Bertoldo, F. Ciardelli, Polymer 45 (26) (2004) 8751.
[28] Cathodeon, Specialist Light Sources.
[29] T.J. Kauppila, T. Kotiako, R. Kostiainen, A.P. Bruins, Journal of the American Society for Mass Spectrometry 15 (2) (2004) 203.
[30] T.J. Kauppila, R. Kostiainan, A.P. Bruins, Analytical Chemistry 74 (21) (2002) 5470.
[31] G.M. Kosolapoff, L. Maier, Organic Phosphorus Compounds, vol. 5, second ed., Wiley-Interscience, New York, Chichester, 1973, p. 329.
[32] L. Bajpai, M. Varshey, C.N. Seubert, S.M. Stevens, J.V. Johnson, R.A. Yost, D.M. Dennis, Journal of the American Society for Mass Spectrometry 16 (6) (2005) 814.
[33] W. Horspool, in: Z. Rappoport (Ed.), The Chemistry of Phenols, John Wiley & Sons, Ltd., 2003, p. 1015.
[34] B. Marcato, M. Vianello, Journal of Chromatography A 869 (1–2) (2000) 285.
[35] K. Schwetlick, W.D. Habicher, in: R. Clough, K. Schwetlick, N. Billingham (Eds.), Polymer Durability: Degradation, Stabilization and Lifetime Prediction, American Chemical Society, Washington, DC, 1995, p. 349.
[36] E. Marotta, R. Seraglia, P. Traldi, International Journal of Mass Spectrometry 228 (2) (2003) 841.
[37] E. Marotta, P. Traldi, Rapid Communications in Mass Spectrometry 17 (24) (2003) 2846.
[38] G. Aksnes, D. Aksnes, Kinetics, Acta Chemica Scandinavica 18 (7) (1964) 1623.
[39] T.N. Novotortzeva, O.B. Kutachinckaya, M.B. Andreeva, E.B. Kalugina, I.L. Aizinson, A.S. Lunin, V.A. Tochin, Y.G. Uranin, I.G. kalinina, K.G. Gumargaliev, G.E. Zaikov, Journal of Applied Polymer Science 76 (6) (2000) 807.
[40] G.J. Klender, in: R. Cough, N. Billingham, K. Gillen (Eds.), Stabilization and Lifetime Prediction, ACS, 1996, p. 397.
[41] G.J. Klender, M.K. Juneau, L.P.T. Burton, W. Kolodahin, Polymer Preprints 34 (2) (1993) 156.
[42] G.J. Klender, in: R. Clough, N. Billingham, K. Gillen (Eds.), Advances in Chemistry Series, ACS, Washington, DC, 1996, p. 397.
[43] M.G. Imajev, Zhurnal Obshchei Khimii 31 (1961) 1762.